Electronic and Spin-Texture Signatures Induced by CO, NO, and O_2 Adsorption on the Bi_2Se_3(0001) Surface

Julián Castro [1] [3], Jorge I. Facio [2], Verónica Vildosola [1]
[1] DFMC, GIyA, CAC, CNEA, INN (CNEA-CONICET); [2] CAB, CNEA and Instituto Balseiro, (CNEA-CONICET); [3] DF-UBA

Abstract: We analyze the adsorption of small molecules on the (0001) surface of Bi_2Se_3 using first-principles density functional theory (DFT) calculations. Specifically, we consider CO, NO, and O_2 adsorbed on a Bi_2Se_3 slab comprising five quintuple layers. Although all these molecules interact weakly with the surface, their highest occupied molecular orbital (HOMO) levels appear at distinct characteristic energies relative to the Fermi level of Bi_2Se_3, reflecting their different reactivities. In particular, the HOMO level of NO lies within the bulk energy gap, favoring direct hybridization with the topological Dirac surface states and modifying their spin–momentum texture. In contrast, the more stable CO and O_2 molecules have their HOMO levels well below the Fermi energy. While both CO and O_2 bonds weaken upon adsorption, CO molecular orbitals hybridize with non-topological Se surface states. These findings provide insight into molecule–surface interactions involving topological states, with potential implications for catalytic applications.

Motivations

- **Bi_2Se_3** preserves **time-reversal symmetry**, which leads to the emergence of protected **surface electronic states** that are **robust against perturbations**, making it a promising candidate for catalytic applications.
- **CO**, **NO**, and **O_2** are **key reactants** in **environmental and energy-related catalytic processes**; therefore, studying their adsorption on this material helps assess its potential application as a catalyst in relevant chemical reactions.

Computational details

- VASP-DFT with the meta-GGA SCAN exchange–correlation functional.
- Valence electrons: Bi ($5d^{10}$ $6s^2$ $6p^3$), Se ($4s^2$ $4p^4$).
- Spin–orbit interaction included in all calculations.
- Energy cutoff: 450–520 eV. k-point grid: 14×14×1 (Bi_2Se_3) with a gaussian smearing of 0.02 eV.
- Force convergence criterion for structural relaxation: 0.02 eV/Å on the top 3 QLs of the slab.
- Becke–Johnson DFT-D3 (van der Waals) scheme.
- Dipole correction applied perpendicular to the surface.

Simulation of bulk

- Tetradymite-type structure, space group R-3m (No. 166).
- Bulk relaxation using the PBE functional does not correctly describe the molecular orbitals (in particular for NO). It underestimates the HOMO–LUMO gap to the point that it becomes comparable with other key energy scales of the system as the Bi_2Se_3 bulk gap and the intermolecular hopping between neighboring molecules. The SCAN functional corrects this, yielding a more consistent energetic hierarchy.

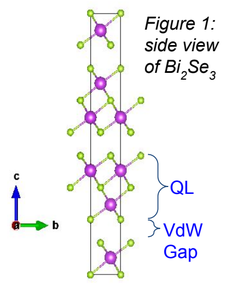

Figure 1: side view of Bi_2Se_3

Simulation of slab

- Slab of 5 QLs for Bi_2Se_3 with 15 Å of vacuum along the direction normal to the surface to avoid hybridization between opposite surface states.
- One molecule adsorbed per unit cell (full coverage) at 3 possible adsorption sites and two orientations (6 cases).
- Site+molecule nomenclature: 1CO, 2NO, $2O_2$, etc.
- Highest stability found at site 2 for the vertical orientation, with the oxygen atom pointing toward the vacuum.

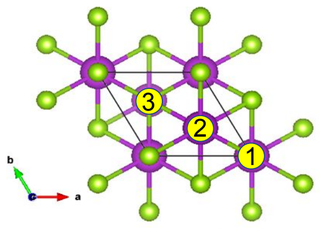

Figure 2: top view of Bi_2Se_3 slab, showing adsorption sites.

Results: band structure and wavefunction projection

- Relaxation with vacuum reduces the **van der Waals (VdW)** gap and the width of the QLs.
- Adsorption energies: −107 meV, −139 meV, and −156 meV for CO, NO, and O_2, respectively.
- The CO and O2 bonds weaken upon adsorption. The expansion of the molecular bond indicates charge transfer toward the corresponding **antibonding orbitals** (0.07 and 0.12 pm, respectively).
- The **bonding HOMO** of CO exhibits hybridization with surface bands localized on the outermost Se atoms and there are no significant changes in the topological states (see Figures 3c and 4).
- O_2 slightly modifies the Se band and its magnetic configuration opens a 3 meV gap at the DP.
- In 2NO, the Fermi level is mainly determined by the band derived from the HOMO of the adsorbed molecule (see Figure 3b). The magnetic moment of NO opens a 2 meV gap at the **Dirac Point (DP)**.
- The **antibonding HOMO** of NO exhibits a 20 meV hybridization gap with the Dirac cone states (see Figure 6b), while its bond length does not change appreciably.

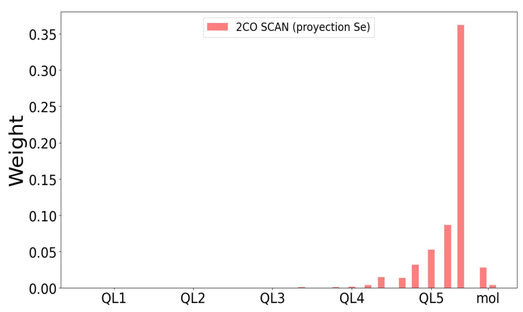

Figure 4: Wavefunction projection of surface Se state (see ★ in figure 3c) on each atomic layer for 2CO system.

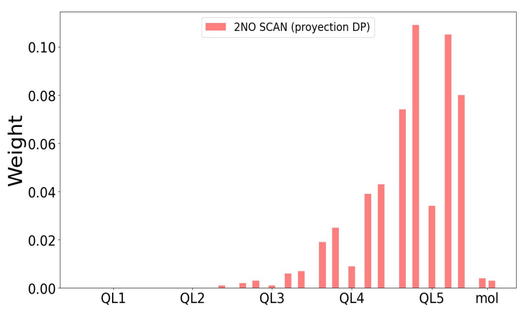

Figure 5: Wavefunction projection of the DP on each atomic layer for 2NO system.

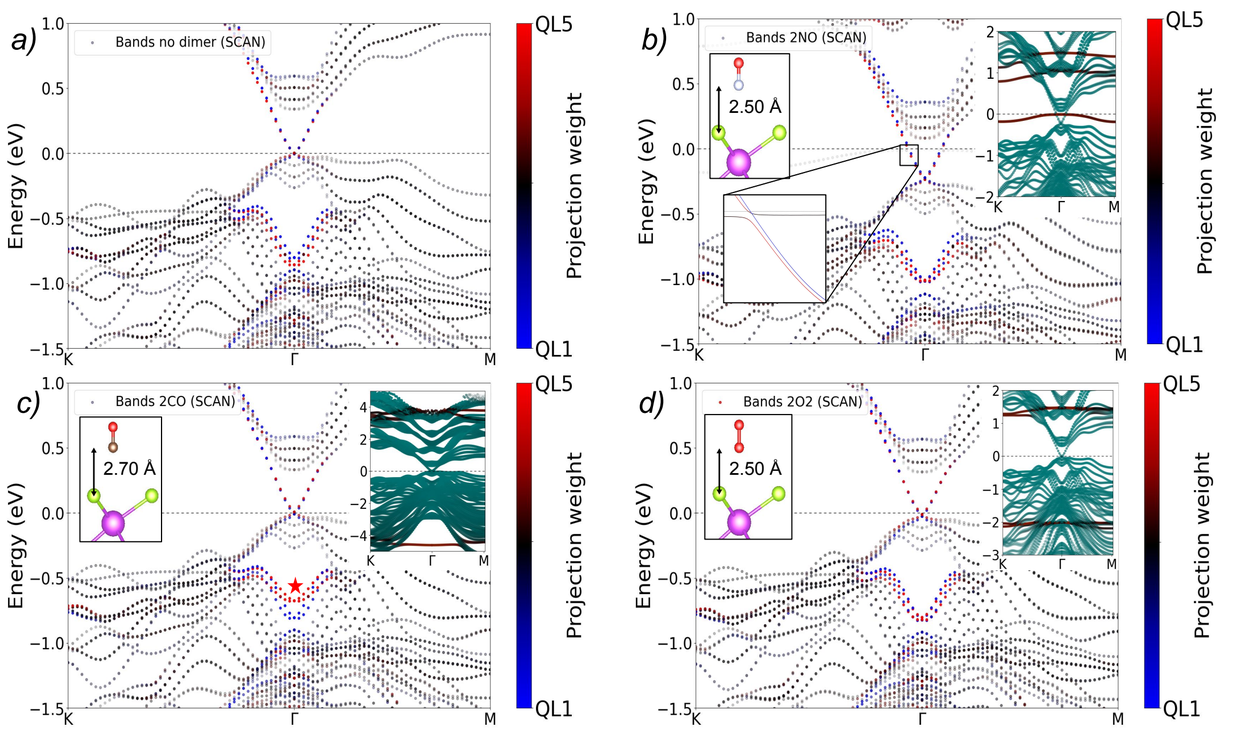

Figure 6: a)-d) Band structure of Bi_2Se_3 without dimer, with NO, CO and O_2, respectively, projected on surface QLs of both sides of the slab. The Fermi level is fixed at 0. Insets of slab bands (turquoise) vs molecular bands (maroon) projections.

Results: spin texture and model Hamiltonian

- Spin texture of the Dirac cone presents:
  - A circular Rashba-like pattern on the xy plane.
  - An oscillating z component far from the origin due to hexagonal warping (see figure 7).
- The spin texture is calculated and plotted in a small section of the Brillouin Zone near the Γ-point ([-0.1, 0.1]x[-0.1, 0.1] in reciprocal vector coordinates, see figure 7).
- The spin components mix and data points of the spin texture near the hybridization are assign based on the weight of their wavefunction on surface QL.
- Near the band crossing:
  - The helical in-plane ($S_{x,y}$) component is suppressed.
  - The out-of-plane (S_z) component from the flat band dominates, causing the spin vectors to align along z.

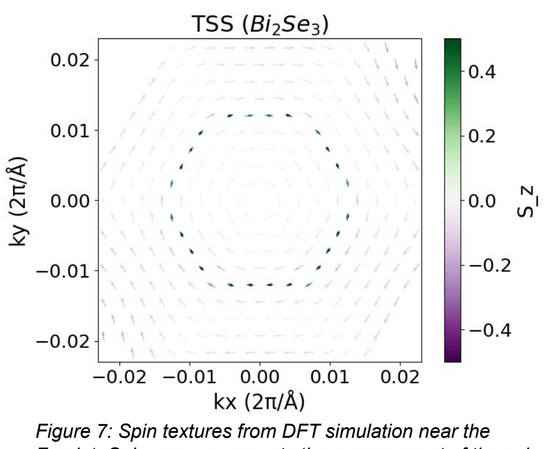

Figure 7: Spin textures from DFT simulation near the Γ-point. Color map represents the z component of the spin.

$$H(k) = \begin{bmatrix} k\sqrt{k^4\lambda^2\sin^2(3\theta) + v^2} & 0 & t \\ 0 & -k\sqrt{k^4\lambda^2\sin^2(3\theta) + v^2} & 0 \\ t & 0 & k^2\alpha + \varepsilon_0 \end{bmatrix}$$

- A simple 3x3 Hamiltonian model with a 2x2 diagonalized Dirac cone Hamiltonian block can be used to describe the hybridization[4].
- Data fitting and band matching through parallel assignment is performed to determine the model parameters and reconstruct the spin texture.

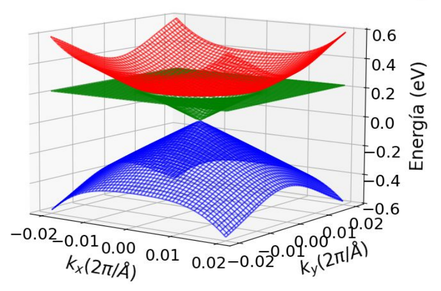

Figure 8: 3 band model Hamiltonian.

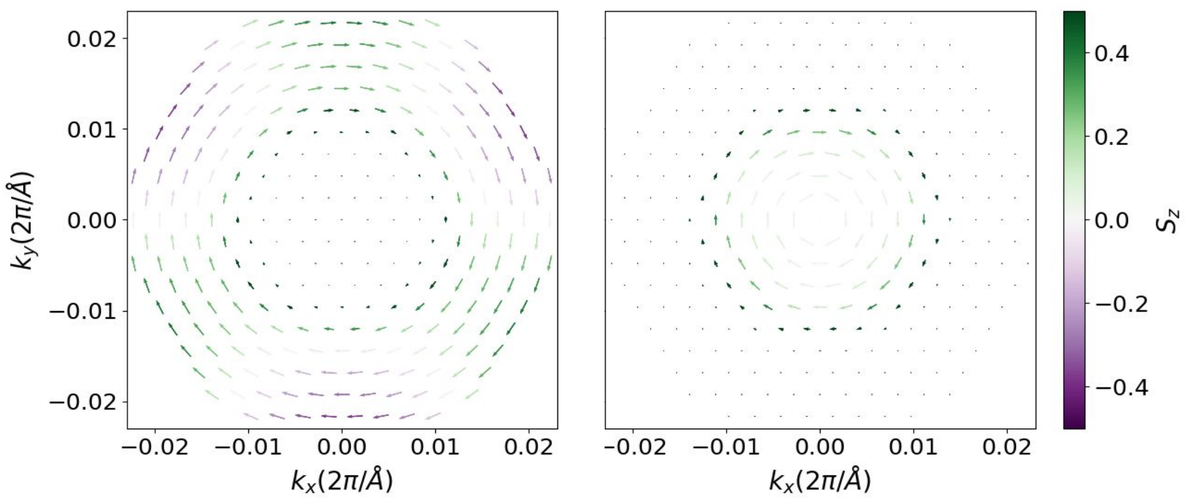

Figure 9: Spin textures from model Hamiltonian. a) Upper hybrid band (red band in figure 8). b) Lower hybrid band (green band in figure 8). Color map represents the z component of the spin.

Conclusions

- ❖ The adsorbed molecules interact weakly with the topological surface states, resulting in charge transfer and bond elongation, with the exception of NO, which doesn't elongate despite hybridizing with the Dirac cone.
- ❖ CO primarily influences the surface non-topological Se-derived states, notably increasing their energy near the Γ point.
- ❖ Oxygen has a smaller impact on the bands near the Fermi level, despite showing a larger binding energy and greater bond expansion.
- ❖ Hybridization with NO induces a canting towards Sz in the spin texture of the Dirac cone near the fermi surface.
- ❖ The 3×3 Hamiltonian with a single hybridizing state reproduces the spin texture qualitatively, showing good agreement with the expected pattern.

References

[1] LI, Jiang, et al. Topological insulator as an efficient catalyst for oxidative carbonylation of amines. Science Advances, 2023, vol. 9, no 38, p. eadh9104.
[2] BIANCHI, Marco, et al. Simultaneous Quantization of Bulk Conduction and Valence States through Adsorption of Nonmagnetic Impurities on Bi_2Se_3. Physical Review Letters, 2011, vol. 107, no 8, p. 086802.
[3] XIE, Ruikuan, et al. Progress, advantages, and challenges of topological material catalysts. Small Science, 2022, vol. 2, no 4, p. 2100106.
[4] Fu, Liang. "Hexagonal warping effects in the surface states of the topological insulator Bi 2 Te 3." Physical review letters 103.26 (2009): 266801.
[5] Bravyi, Sergey, David P. DiVincenzo, and Daniel Loss. "Schrieffer–Wolff transformation for quantum many-body systems." Annals of physics 326.10 (2011): 2793-2826.